*Metrol. Meas. Syst.*, Vol. XVIII (2011), No. 1, pp. 00-00

PAN POLSKA AKADEMIA NAUK

METROLOGY AND MEASUREMENT SYSTEMS

Index 330930, ISSN 0860-8229

*www.metrology.pg.gda.pl*

M&MS

# ANALYSIS OF THE FACTORS AFFECTING THE REALIZATION OF LAMBDA TRANSITION TEMPERATURE OF $^4$HE

**L. Yin[1)], P. Lin[2)], J. J. Zhao[1)] and X. Qi[1)]**

*1) School of Science, Beijing University of Chemical Technology, Beijing 100029, China (yinliang@mail.buct.edu.cn, zhaojingjing2345@126.com, ✉qixin@mail.buct.edu.cn, +86 10 64433867)*

*2) Division of Thermometry and Materials Evaluation, National Institute of Metrology, Beijing 100013, China (linp@nim.ac.cn)*

**Abstract**

Owing to the dramatic change in the thermal conductivity of $^4$He when its temperature crosses the transition of superfluid (HeI) and normalfluid (HeII), a sealed-cell with a capillary is used to realize the lambda transition temperature, $T_\lambda$. A small heat flow is controlled through the capillary of the sealed-cell so as to realize the coexistence of HeI and HeII and maintain the stay of HeI/HeII interface in the capillary. A stable and flat lambda transition temperature "plateau" is obtained. Because there is a depression effect of $T_\lambda$ caused by the heat flow through the capillary, a series of heat flows and several temperature plateaus are made and an extrapolation is applied to determine $T_\lambda$ with zero heat flow. A rhodium-iron resistance thermometer with series number A34（RIRT A34）has been used in 24 $T_\lambda$ -realization experiments to derive $T_\lambda$ with a standard deviation of 0.022mK, which proves the stability and reproducibility of $T_\lambda$.

Keywords: $^4$He, lambda transition temperature, sealed-cell, realization



## 1. Introduction

The temperature scale consists of temperature fixed points, interpolating instruments and formulas. The temperature fixed point plays an important role in establishing a temperature scale because of the advantages of accurate value, perfect reproducibility and small temperature drift over time. The International Temperature Scale of 1990(ITS-90) was established by interpolating a series of defined temperature fixed points with a standard platinum resistance thermometer in the temperature range between 13.8K and 1234K. In ITS-90 [1], the lowest temperature fixed point is the hydrogen triple point temperature, 13.8033K, whose thermodynamic temperature uncertainty is 0.5mK and the best practical reproducibility is 0.1mK. There is no defined temperature fixed point under 13.8033K.

In ITS-90, the lambda transition temperature of $^4$He at the saturated vapor pressure is 2.1768K [1]. In 1976, Hwang and Khorana reported a typical reproducibility of 0.01mK for the lambda transition by pumping a pool of $^4$He in order to cool it down through the lambda transition temperature and they suggested that the lambda point of liquid helium could be used as temperature fixed point [2]. In 1992, Duncan and Ahlers reported the utilization of a $^4$He superfluid-transition fixed-point device to realize the superfluid transition temperature. Using this device they averred that $T_\lambda$ can reach a level of $10^{-8}$K [3].

From 1990 to 2003, our research team reported the realization of the lambda transition temperature of $^4$He with a new sealed-cell. A small heat flow was controlled to maintain the stay of HeI/HeII interface in the capillary of the sealed-cell, and an extrapolation was used to determine the lambda transition temperature with zero heat flow [4–7].

Article history: received on Nov. 16, 2010; accepted on Jan. 10, 2011; available online on Mar. 21, 2011.

In order to improve the accuracy of the $T_\lambda$ -realization and to prove the stability and reproducibility of $T_\lambda$, two new sealed-cells were made and 24 $T_\lambda$ -realization experiments have been performed at the Chinese National Institute of Metrology. First, the experimental devices and principles were introduced, followed by the experimental methods and results. Next, the depression effect of $T_\lambda$ caused by the heat flow through the capillary of the sealed-cell and the factors affecting the results of $T_\lambda$ -realization experiments were discussed and conclusions drawn. The standard deviation of 24 $T_\lambda$ -realization experiments is 0.022mK, which proves the stability and reproducibility of $T_\lambda$.

## 2. Experimental description

### *2.1. Experimental devices*

*The sealed-cell*

The sealed-cell used in the $T_\lambda$ -realization experiments consists of four parts: the variable-temperature platform, the top chamber, the stainless steel capillary and the bottom chamber, as shown in Fig. 1. The sealed-cell is filled with high-pressure helium gas at room temperature. When the temperature of the sealed-cell is cooled below $T_\lambda$, the bottom chamber, the capillary and the bottom of the top chamber become filled with HeII. The temperature of the bottom chamber and the variable-temperature platform is then controlled to realize the coexistence of HeI and HeII in the capillary. HeI appears in the bottom chamber and the lower part of the capillary, while HeII exists in the upper part of the capillary and the bottom of the top chamber. Because of the self-adjusting effect of the HeI liquid column in the capillary, the stay of HeI/HeII interface in the capillary is maintained, and the temperature of the HeI/HeII interface is $T_\lambda$.

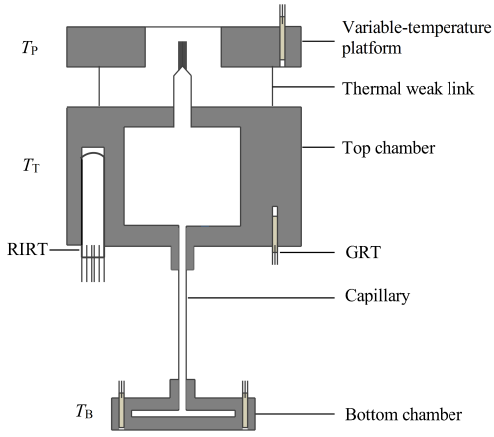


Fig. 1. Sealed-cell for the realization experiment.

Because of the large thermal conductivity of HeII, the temperature measured by the RIRT installed in the top chamber of the sealed-cell, $T_T$, is very close to the HeI/HeII interface temperature, $T_\lambda$.

Five sealed-cells are used in the $T_\lambda$ -realization experiments and the basic data are listed in Table 1. The capillary dimension of the sealed-cell D2 is different from others in order to detect the influence of the capillary size on the $T_\lambda$ -realization experiment.

Table 1. Basic data of the five sealed-cells for the $T_\lambda$ -realization experiments.

| Cell number | Outer diameter of the capillary, mm | Wall thickness of the capillary, mm | Length of the capillary, mm | Outer diameter of the top chamber, mm | Fill pressure, MPa | Sealing date |
|---|---|---|---|---|---|---|
| C3 | 3 | 0.5 | 40 | 42 | 10.5 | 2000/3 |
| D1 | 3 | 0.5 | 40 | 42 | 10 | 2000/6 |
| D2 | 3 | 0.5 | 47 | 42 | 10 | 2000/6 |
| L1 | 3 | 0.5 | 40 | 42 | 10 | 2009/4 |
| L2 | 3 | 0.5 | 40 | 42 | 10 | 2009/4 |

*Thermometers and measuring instruments used in the $T_\lambda$ -realization experiments*

Five RIRTs used in the $T_\lambda$ -realization experiments were made by Tinsley and calibrated by NPL from 1977 to 1985 with an uncertainty of less than 1mK. The calibration table of 5 RIRTs is converted to the ITS-90 and the calibration values approaching $T_\lambda$ are listed in Table 2.

Five RIRTs are installed in the top chamber of the sealed-cell. RIRT A34 is used as a master thermometer to record the realization temperature and the other RIRTs are compared with the master thermometer.

Table 2. Calibration values of 5 RIRTs close to 2.1768K.

| Thermometer serial number | Resistance, Ω | Corresponding temperature, K | Sensitivity, K/Ω |
|---|---|---|---|
| A20 | 3.035 | 2.1764 | 3.27 |
| A34 | 2.395 | 2.1689 | 4.33 |
| A35 | 2.600 | 2.1694 | 3.98 |
| 229841 | 2.975 | 2.1663 | 3.20 |
| 229843 | 3.014 | 2.1722 | 3.23 |

The system block diagram of the $T_\lambda$ -realization experiment is shown in Fig. 2. The following instruments are included : An ASL F18 AC bridge to measure the RIRT's resistance, two Lake Shore 332 Temperature Controllers to control the temperature of the variable-temperature platform and the bottom chamber and measure the heating power of the bottom chamber, a Keithley 6220 Precision Current Source and an Agilent 3458A High Performance Digital Multi-meter to measure the resistance of the Germanium resistance thermometer (GRT) which is installed in the sealed-cell.

The resistance resolution of the F18 AC bridge is 1 μΩ with a 10Ω standard resistor, which is equivalent to a temperature resolution of 3.2μK at 2.17 K.

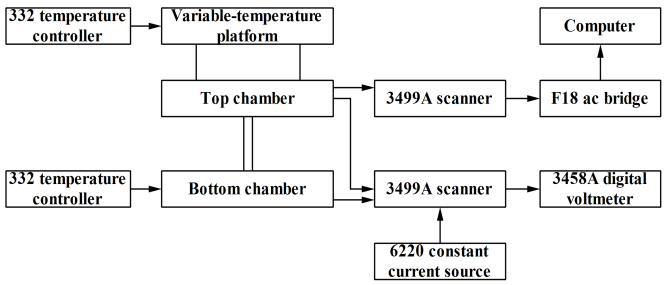


Fig. 2. System block diagram of the $T_\lambda$ -realization experiment.

### 2.2. Experimental principle

#### 2.2.1. Self-adjusting effect of HeI liquid column in the capillary

The temperature of the bottom chamber, $T_B$, is set to a value that is about 10mK higher than $T_\lambda$ and the temperature of the variable-temperature platform, $T_p$, is set to a certain value below $T_\lambda$. So the temperature of the liquid helium in the capillary crosses $T_\lambda$. The stay of the HeI/HeII interface in the capillary is maintained at a certain point and the temperature of the HeI/HeII interface is $T_\lambda$.

Fig. 3 shows the distribution of the temperature and the heat flow in the sealed-cell. From the analysis of the thermal state of the liquid helium in the sealed-cell, the thermal conductivity of HeII above the HeI/HeII interface is so large that the temperature difference along the HeII liquid column is very small. Hence, the temperature of HeII in the top chamber, $T_T$, is very close to the temperature of the HeI/HeII interface， $T_\lambda$.

In this state, if the stray heat leaks from the 4.2K cryostat wall to the sealed-cell and the self-heating effect of the RIRT are neglected, the heat flow through the capillary, $Q_C$, is equal to the heat flow from the top chamber to the variable-temperature platform, $Q_{TP}$, and they are all equal to the heating power of the bottom chamber, $P_B$, which we purposely introduce to the bottom chamber to compensate for the heat loss $Q_C$:

$$Q_C = Q_{TP} = P_B . \tag{1}$$

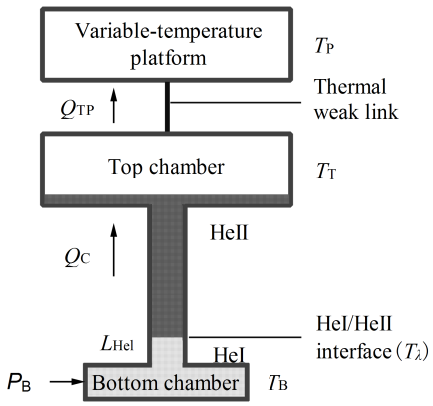


Fig. 3. Distribution of the temperature and the heat flow in the sealed-cell.

Under stationary conditions, the heat flow, $Q_{TP}$, is proportional to the temperature difference between the top chamber and the variable-temperature platform:

$$Q_{TP} = \lambda_{CuI} S_{CuI} (T_T - T_P)/L_{CuI} , \tag{2}$$

where: $Q_{TP}$ = heat flow from the top chamber to the variable-temperature platform, W; $\lambda_{CuI}$=thermal conductivity of the copper rods between the top chamber and the platform, W/(m·K); $S_{CuI}$ =cross-sectional area of the copper rods between the top chamber and the platform, m$^2$; $L_{CuI}$ =length of the copper rods between the top chamber and the platform, m.

As $T_T$ remains constant, $T_p$ is regulated to control $Q_{TP}$ and $Q_C$ simultaneously (See equations 1 and 2).

The heat state of the HeI liquid column in the capillary is shown in equation 3.

$$Q_C = \lambda_{HeI} S_{He} (T_B - T_T) / L_{HeI} \ , \tag{3}$$

where $\lambda_{HeI}$ = thermal conductivity of HeI in the capillary, W/(m·K); $S_{He}$ = cross-sectional area of the helium column in the capillary, $m^2$; $L_{HeI}$ =height of the HeI column in the capillary, m.

When $T_B$ is fixed and $T_p$ is increased (say from 20 to 30 mK), the heat flow $Q_C$ will decrease (See equation 2) and the height of HeI liquid column in the capillary $L_{HeI}$, will increase (See equation 3).

As long as $L_{HeI}$ is shorter than the capillary length, no matter how high $T_P$ is, the HeI/HeII interface always remains in the capillary. The adjustment in height of HeI liquid column in the capillary automatically compensates for the change of the heat flow, $Q_C$. This is the self-adjusting effect of HeI liquid column in the capillary.

#### *2.2.2. The depression effect of $T_\lambda$ caused by the heat flow through the capillary*

Because of the depression effect of $T_\lambda$ caused by the heat flow $Q_C$, $T_\lambda$ increases with the decrease of $Q_C$ in the realization experiments. The temperature set point of $T_p$ is increased stepwise (typically 20 to 30 mK in each step), and then the heat flow $Q_C$ correspondingly decreases as $T_T$ gradually increases. As a result, a series of the temperature plateaus of $T_T$ are obtained. Then, an extrapolation is used to determine $T_\lambda$ with zero heat flow to correct the depression effect of $T_\lambda$ and other influences related to the heat flow.

### *2.3. Methods of $T_\lambda$ -realization experiment*

The vacuum can of the thermostat is pumped to a state of vacuum which should be better than $10^{-3}$Pa at room temperature. Then the 1K pot of the thermostat is pumped in order to cool it down. After the temperature of the sealed-cell is cooled down below $T_\lambda$, the temperature of the bottom chamber and the platform is controlled, and the temperature plateau of $T_T$ can be obtained in the top chamber.

When the temperature set point of $T_p$ is increased, $Q_C$ decreases and $T_T$ increases to a new plateau. Each lambda transition temperature plateau has been computer-recorded for 15 minutes and a series of step temperature plateaus of lambda transition can be obtained by steadily increasing $T_p$. Subsequently, an extrapolation is used to determine $T_\lambda$ with zero heat flow.

### *2.4. $T_\lambda$ -realization experimental results*

#### *2.4.1. A typical experimental data and curves*

24 $T_\lambda$ -realization experiments have been performed. Table 3 shows a typical $T_\lambda$ -realization data of the sealed-cell L-2.

Table 3. A typical experimental data of the sealed-cell L-2.

| Heat flow $Q_C$, μW | Top chamber temperature $T_T$, K | Platform temperature $T_p$, K | Heat flow $Q_C$, μW | Top chamber temperature $T_T$, K | Platform temperature $T_p$, K |
|---|---|---|---|---|---|
| 121.3 | 2.176916 | 2.0492 | 31.2 | 2.177184 | 2.1502 |
| 91.9 | 2.177006 | 2.0827 | 22.4 | 2.177224 | 2.1602 |
| 73.2 | 2.177056 | 2.1037 | 7.7 | 2.177269 | 2.1757 |
| 56.9 | 2.177096 | 2.1219 | 31.3 | 2.177184 | 2.1507 |
| 44.2 | 2.177144 | 2.1361 | | | |

A typical plot of $T_T$ versus $Q_C$ is drawn as seen in Fig. 4 and it can be fitted linearly. The curvilinear equation is:

$$T_T = -0.00000308\ Q_C + 2.17728417\ . \tag{4}$$

The depression coefficient of $T_\lambda$, $h$, is the slope of this curve which is about -3.08μK/μW. By extrapolating this curvilinear equation to $Q_C = 0\mu W$, the value of $T_T$ with no heat flow depression is obtained, i.e., $T_T$ = 2.177284 K.

The formula of the self-heating effect of the RIRT is:

$$\Delta T_{SH} = (T_{0.5} - T_{0.28}) \times 0.28^2 / (0.5^2 - 0.28^2), \tag{5}$$

where $\Delta T_{SH}$ = self-heating value of the RIRT at 0.28mA measuring current, K; $\Delta T_{0.5}$ = temperature of the RIRT measured with 0.5mA measuring current, K; $\Delta T_{0.28}$ = temperature of the RIRT measured with 0.28mA measuring current, K.

After correcting the influence of the self-heating effect of the RIRT, the $T_\lambda$ -realization value is 2.176972K.

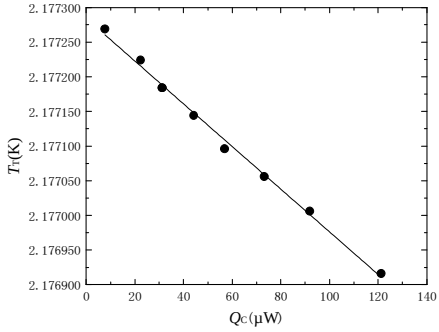


Fig. 4. A typical plot of $T_T$ versus $Q_C$ for the sealed-cell L2.

### *2.4.2. Results of 24 $T_\lambda$ -realization Experiments*

The lambda transition temperatures of 24 realization experiments recorded by RIRT A34 are listed in Table 4. All the realization temperatures are extrapolated to zero heat flow and the self-heating effect of the RIRT deducted. The lowest value of the realization temperatures is 2.176909K and the highest is 2.176988K. The difference is 0.079mK. The average value of 24 $T_\lambda$ -realization experiments is 2.176948K and the standard deviation is 0.022mK.

Table 4. The lambda transition temperatures of 24 realization experiments recorded by RIRT A34.

| Serial number | Date | Cell | Master thermometer | Recorded by RIRT A34, K | Difference , mK |
|---|---|---|---|---|---|
| 1 | 2008-11-25 | D2 | A20 | 2.176924 | -0.024 |
| 2 | 2008-12-11 | D2 | A20 | 2.176924 | -0.024 |
| 3 | 2008-12-12 | D2 | A34 | 2.176939 | -0.009 |
| 4 | 2008-12-23 | C3 | A34 | 2.176933 | -0.015 |
| 5 | 2008-12-24 | C3 | A34 | 2.176938 | -0.010 |
| 6 | 2008-12-25 | C3 | A34 | 2.176932 | -0.016 |
| 7 | 2009-2-24 | C3 | A34 | 2.176946 | -0.002 |
| 8 | 2009-2-25 | C3 | A34 | 2.176956 | 0.008 |
| 9 | 2009-2-26 | C3 | A34 | 2.176957 | 0.009 |
| 10 | 2009-2-27 | C3 | A34 | 2.176949 | 0.001 |
| 11 | 2009-3-20 | D1 | A34 | 2.176917 | -0.031 |
| 12 | 2009-3-24 | D1 | A34 | 2.176933 | -0.015 |
| 13 | 2009-3-25 | D1 | A34 | 2.176931 | -0.017 |
| 14 | 2009-3-26 | D1 | A34 | 2.176935 | -0.013 |
| 15 | 2009-3-27 | D1 | A34 | 2.176909 | -0.039 |
| 16 | 2009-5-7 | L2 | A34 | 2.176954 | 0.006 |
| 17 | 2009-5-8 | L2 | A34 | 2.176954 | 0.006 |
| 18 | 2009-5-13 | L2 | A34 | 2.176964 | 0.016 |
| 19 | 2009-5-14 | L2 | A34 | 2.176972 | 0.024 |
| 20 | 2009-5-15 | L2 | A34 | 2.176956 | 0.008 |
| 21 | 2009-5-20 | L1 | A34 | 2.176983 | 0.035 |
| 22 | 2009-5-21 | L1 | A34 | 2.176985 | 0.037 |
| 23 | 2009-5-22 | L1 | A34 | 2.176988 | 0.040 |
| 24 | 2009-12-16 | L2 | A34 | 2.176967 | 0.019 |
| Average for 24 realizations, K | | | | 2.176948 | |
| Stand deviation, mK | | | | | 0.022 |

The results of 24 $T_\lambda$ -realization experiments with RIRT A34 are shown in Fig. 5. We can find that the realization values of different sealed-cells show a few deviations. The realization temperature of sealed-cell D2 has no difference from the other sealed-cells although its capillary is shorter than the other sealed-cells.

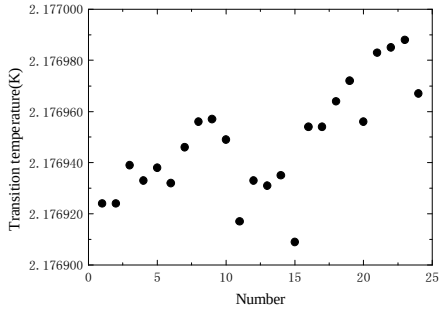


Fig. 5. The results of 24 $T_\lambda$ -realization experiments with RIRT A34.

## 3. Analysis of factors affecting the $T_\lambda$ -realization experiment

### *3.1. Factors affecting the depression effect of $T_\lambda$ caused by the heat flow through the capillary*

The depression effect of $T_\lambda$ caused by the heat flow through the capillary, $Q_C$,is obvious and the depression coefficient is -3.08μK/μW in the typical experiment as shown in Section *2.4.1*. The factors affecting the depression effect are analyzed as follows.

#### *3.1.1. The heat flow through the HeI/HeII interface*

Duncan reported that the heat flow through the HeI/HeII interface which is equal to $Q_C$ depresses $T_\lambda$ by an amount [8]:

$$\Delta T_\lambda / T_\lambda = \left(q_C / q_0\right)^X , \tag{6}$$

where $\Delta T_\lambda =$ depression value of $T_\lambda$ caused by the heat flow through the HeI/HeII interface, K; $q_0 = 568 \pm 200 W/cm^2$; $X = 0.813 \pm 0.012$; $q_C = Q_C / S_{He}$.

When $Q_C = 100 \mu W$, we can arrive at $\Delta T_\lambda \approx 117 \mu K$ and the impact on $T_\lambda$ is negative.

#### *3.1.2. The temperature difference along the HeII column*

Despite the thermal conductivity of HeII which is many orders of magnitude larger than that of HeI [9, 10], a 100μW heat flow also produces a temperature difference along the HeII liquid column.

The temperature difference between the top chamber and the bottom chamber is 7mK in a typical experiment as shown in Section *2.4.1*. From equation 3, we can figure out that $L_{HeI}$ is 0.047mm. Thus, the capillary is almost filled with the HeII liquid column which is about 4cm high. The temperature difference along the HeII liquid column is:

$$\Delta T_{HeII} = Q_C L_{HeII} / \lambda_{HeII} S_{He} , \tag{7}$$

where: $\Delta T_{HeII} =$ temperature difference along the HeII column in the capillary, K; $L_{HeII} =$ height of the HeII column in the capillary, m; $\lambda_{HeII} =$ thermal conductivity of HeII, W/(m·K).

When $Q_C = 100 \mu W$, $\Delta T_{HeII} \approx 130 \mu K$ is obtained and the impact on $T_\lambda$ is negative.

#### *3.1.3. Kapitza resistance*

Kapitza resistance exists when heat flows across the interface between the liquid helium layer and the solid endplate [11]. The thermal resistance coefficient of the copper surface of the top chamber, $R_K$, may be up to 2cm$^2$K/W in our realization experiment. Because of the creeping film effect of HeII, it is assumed that all the inner surface of the top chamber is covered with HeII membrane and the Kapitza resistance is:

$$\Delta T_K = Q_C R_K / S_A , \tag{8}$$

where $\Delta T_K =$ Kapitza resistance between the liquid helium layer and the solid endplate, K; $S_A =$ inner surface area of the top chamber, m$^2$.

When $Q_C = 100\mu W$, we can obtain $\Delta T_K \approx 8\mu K$. If the HeII membrane only covers the lower surface of the top chamber, the Kapitza resistance is 64μK and the impact on $T_\lambda$ is negative.

### *3.1.4. Temperature gradient along the copper wall of the top chamber*

If all the heat flow coming from the capillary goes through the copper wall of the top chamber to the variable-temperature platform, a temperature difference, $\Delta T_{Cu}$, exists along the copper wall of the top chamber whose ring cross-sectional area is 9.5cm$^2$, and the height of the temperature gradient along the top chamber is approximately equal to the length of the RIRT, which is 3cm. The temperature gradient along the copper wall of the top chamber is:

$$\Delta T_{Cu} = Q_C L_{CuII} / \lambda_{CuII} S_{CuII}, \tag{9}$$

where $\Delta T_{Cu} =$ temperature difference along the copper wall of the top chamber, K; $L_{CuII} =$ height of the copper wall of the top chamber, m; $\lambda_{CuII} =$ thermal conductivity of the copper wall of the top chamber, W/(m·K); $S_{CuII} =$ ring cross-sectional area of the copper wall of the top chamber, m$^2$.

The maximum temperature difference generated by a 100μW heat flow is about 16μK. The impact on $T_\lambda$ is negative.

In conclusion, if $Q_C = 100\mu W$, the total factor depressing $T_\lambda$ is:

$$\Delta T \approx \Delta T_\lambda + \Delta T_{HeII} + \Delta T_K + \Delta T_{Cu} \approx -271\mu K, \tag{10}$$

where $\Delta T =$ total factors depressing $T_\lambda$ for the theoretical value, K.

This is consistent with the experimental data of -3.0μ8K/μW in the typical experiment as shown in Section *2.4.1*. These factors can be corrected by extrapolating to zero heat flow.

### *3.2. Factors affecting the precision of the $T_\lambda$ -realization experiment*

### *3.2.1. The temperature fluctuation of the platform*

The result of the $T_\lambda$ -realization experiment is influenced by the temperature stability of the platform. A typical plot of $T_T$ versus $T_p$ (for the typical experiment as shown in Section *2.4.1*) is seen in Fig. 6 and it can be fitted linearly. The curvilinear equation is:

$$T_T = 0.002757 T_P + 2.171259. \tag{11}$$

We can obtain $dT_P / dT_T \approx 363$ from the equation, suggesting that the temperature fluctuation of $T_T$ is about 1/363 of the temperature fluctuation of $T_T$. In the realization experiments, the fluctuation of $T_p$ is controlled below 1 mK, thus having a less than 3μK impact on $T_T$.

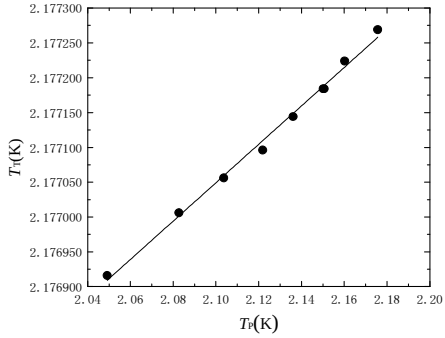


Fig. 6. A typical plot of $T_T$ versus $T_p$ for the sealed-cell L2.

### *3.2.2. Stray heat leaks*

The radiation heat leak and the residual helium gas heat leak from the 4.2K cryostat wall to the sealed-cell in the experiments influence the experimental results.

A typical plot of $P_B$ versus $T_p$ (for the typical experiment as shown in Section *2.4.1*) is drawn in Fig. 7 and it can be fitted linearly. The curvilinear equation is:

$$P_B = -895.8T_P + 1957.5 . \tag{12}$$

By extrapolating to $T_P = 2.1768K$, we can get $P_B \approx 7.5\mu W$, which is equal to the stray heat leaks from the 4.2K cryostat wall to the sealed-cell. The depression coefficient of $T_\lambda$ caused by the heat flow is -3.08μK/μW (for the typical experiment as shown in Section *2.4.1*), so the impact of the stray heat leaks on $T_\lambda$ is $\Delta T_S \approx -3.08\mu K/\mu W \times 7.5\mu W \approx -23\mu K$, where $\Delta T_S =$ influencing value of $T_\lambda$ by the stray heat leaks, K.

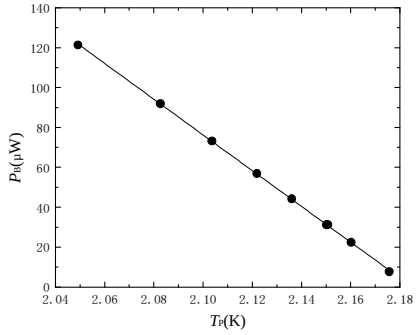


Fig. 7. A typical plot of $P_B$ versus $T_p$ for the sealed-cell L2.

### *3.2.3. HeII liquid column static pressure*

The HeII liquid column in the capillary creates a static pressure on the HeI/HeII interface [12, 13], which influences the $T_\lambda$ -realization experimental results. Ahlers reported that the correction factor of the liquid helium static pressure is -1.27μK/cm [13]. In this experiment, the position of the liquid-vapor interface is about 4cm above the HeI/HeII interface, so the

HeII liquid column static pressure has an impact on $T_\lambda$ -realization experimental results, $\Delta T_L \approx -1.27\mu K/cm \times 4cm \approx -5.08\mu K$, where $\Delta T_L =$ influencing value of $T_\lambda$ by HeII liquid column static pressure, K.

## 4. Conclusions

A sealed-cell with a capillary and an extrapolation method was used to realize the lambda transition temperature, $T_\lambda$. The average value of 24 realization experiments for the lambda transition temperature of $^4$He is 2.176948K and the standard deviation is 0.022mK. The depression effect of $T_\lambda$ caused by heat flow through the capillary was analyzed and the theoretical value is highly consistent with the experimental data.

The experimental results prove the stability and reproducibility of $T_\lambda$. It is recommended the lambda transition temperature of $^4$He be used as the fixed point of the International Temperature Scale.

## References


[1] Thomas, H.P. (1990). The International Temperature Scale of 1990, (ITS-90). *Metrologia*, 27, 3-10.

[2] Hwang, K.F., Khorana, B.M. (1976). Lambda transition of liquid helium as a thermometric fixed point. *Metrologia*, 12, 61-63.

[3] Duncan, R.V., Ahlers, G. (1992). A sealed $^4$He superfluid-transition fixed-point device. In *Temperature, its Measurement and Control in Science and Industry*. American Institute of Physics. New York, 243-245.

[4] Lin, P., Mao, Y.Z., Hong, C.S., Yue, Y., Zhang, Q.G. (1990). Study of the realization of $^4$He lambda transition point temperature by means of a small sealed cell. *Cryogenics*, 30, 432-436.

[5] Lin, P., Mao, Y.Z. , Yu, L.H., Zhang, Q.G., Hong, C.S. (2002). Studies on a sealed-cell lambda-point device for use in low temperature thermometry. *Cryogenics*, 42, 443-450.

[6] Peroni, I., Pavese, F., Ferri, D., Lin, P., Zhang, Q.G., Yu, L. H. (2002). A sealed cell for the accurate realization of the λ-point of $^4$He, In: *Proceedings of TEMPMEKO 2001, 8th International Symposium on Temperature and Thermal Measurements in Industry and Science.* VDE Verlag GMBH. Berlin, 391-396.

[7] Lin, P., Mao, Y.Z., Hong, C.S., Pavese, F., Peroni, I., Head, D., Rusby, R. (2003). Realization of the lambda transition temperature of $^4$He using sealed cells. In: *Temperature, its Measurement and Control in Science and Industry*. American Institute of Physics. New York, 191-195.

[8] Duncan, R.V., Ahlers, G., Steinberg, V. (1988). Depression of the superfluid transition temperature in $^4$He by a heat current. *Physical Review Letters*, 60, 1522-1525.

[9] Kerrisk, J., Keller, W. (1969). Thermal Conductivity of Fluid $^3$He and $^4$He at Temperatures between 1.5 and 4.0° K and for Pressures up to 34 atm. *Physical Review*, 177, 341-351.

[10] Ahlers, G. (1968). Thermal conductivity of HeI near the superfluid transition. *Physical Review Letters*, 21, 1159-1162.

[11] Pollack, G.L. (1969). Kapitza Resistance. *Rev. Mod. Phys.*, 41, 48-81.

[12] Kierstead, H.A. (1967). Lambda Transformation of Liquid $^4$He at High Pressures. *Physical Review*, 153, 258-262.

[13] Ahlers, G. (1968). Effect of the gravitational field on the superfluid transition in $^4$He. *Physical Review*, 171, 275-282.